Intershell Exchange and Sequential Electrically Injected Spin Populations of InAs Quantum-Dot Shell States

G. Kioseoglou,[1,4,*] M. Yasar,[2] C. H. Li,[1] M. Korkusinski,[3] M. Diaz-Avila,[2] A. T. Hanbicki,[1] P. Hawrylak,[3] A. Petrou,[2] and B. T. Jonker[1,*]

[1]*Naval Research Laboratory, Washington, District of Columbia, 20375, USA*
[2]*Department of Physics, 239 Fronczak Hall, University at Buffalo, Buffalo, New York 14260, USA*
[3]*Quantum Theory Group, Institute for Microstructural Sciences, National Research Council, Ottawa, Canada K1A0R6*
[4]*Department of Materials Science and Technology, University of Crete, Heraklion Crete, 71003, Greece*

(Received 16 July 2008; published 26 November 2008)

We report sequential spin population of individual shell states of self-assembled InAs quantum dots controlled by a spin-polarized current from an Fe contact, and determine the *s*-*p* and *p*-*d* intershell exchange energies. We resolve excitonic features in the electroluminescence (EL) spectra associated with individual quantum levels. In contrast with simple models of shell occupation, the EL circular polarization exhibits maxima shifted with respect to the intensity peaks. Calculations show that this is due to intershell exchange. Exchange energies for the *s*-*p* and *p*-*d* shells are 7 ± 2 and 13.5 ± 1 meV, respectively.

DOI: 10.1103/PhysRevLett.101.227203 PACS numbers: 85.75.−d, 78.67.Hc

Many spintronic and quantum computing applications, including spin transistors, spin-based quantum processors, memory devices and polarized light emitters [1–6] require efficient injection of spin-polarized carriers into specific quantum levels of nanoscale semiconductor structures. Quantum dots (QDs) are attractive candidates for these applications, because their reduced dimensionality leads to long spin coherence times [7,8] and enables the localization and manipulation of a controlled number of electrons [9–13]. QDs are often referred to as ''artificial atoms'' since their electronic structure is described using the *s*, *p*, *d*, *f* shell nomenclature used for atoms [9,14]. Previous work has described electrical spin injection into ensembles of InAs QDs incorporated into *p*-*i*-*n* light emitting diodes (LEDs) from ferromagnetic GaMnAs [15], from paramagnetic ZnMnSe layers [16], and from ferromagnetic metal contacts [17,18]. The electroluminescence (EL) from these studies consisted of a single broad feature associated with transitions among the lowest energy QD states. The large width of the emission band was attributed to inhomogeneous size distribution of the QDs.

We present here EL data from Fe/*n*-AlGaAs/*i*-GaAs/*p*-AlGaAs spin-LEDs that incorporate a single layer of InAs QDs at the center of a GaAs quantum well (QW). In contrast with previous work, we resolve excitonic features in the EL spectra associated with individual quantum levels (*s*, *p*, *d*, and *f* shells). We demonstrate electrical control of the electron population and spin polarization of these shells with bias current, and determine values for the *s*-*p* and *p*-*d* intershell exchange energies. Intershell exchange strongly modifies the optical polarization observed from that expected for simple models of shell occupation. The polarization of the EL spectra exhibits maxima that do not coincide with the EL intensity peaks, contrary to what one would expect from a simple excitonic picture. Calculations show that these energy shifts arise from exchange interactions among spin-polarized multiexciton complexes in a QD. The experimental data together with these calculations yield values for the average exchange energies of electrons in the *s* and *p* shells, $V_X(sp) = 7 \pm 2$ meV, and between electrons in the *p* and *d* shells, $V_X(pd) = 13.5 \pm 1$ meV. These results are significant to our fundamental understanding of spin-polarized carriers in QDs, and indicate a mechanism for electrical control of spins in QDs for their various spin-based applications.

Samples were grown by molecular beam epitaxy (MBE) and consist of a QW structure [17,19] of 83 nm *n*-$Al_{0.1}Ga_{0.9}As$/40 nm undoped GaAs/50 nm *p*-$Al_{0.3}Ga_{0.7}As$/*p*-GaAs buffer layer on a *p*-GaAs (001) substrate. The top 15 nm of *n*-type $Al_{0.1}Ga_{0.9}As$ was highly doped ($n = 1 \times 10^{19}$ cm^{-3}) to form a Schottky tunnel contact to facilitate spin injection from the Fe film [20,21]. The top 10 nm Fe (001) film was grown in a separate interconnected MBE chamber. The self-assembled InAs QD layer, grown at 500 °C at a reduced growth rate of 0.001 ML/ sec to reduce the dot density and size distribution [22], was embedded at the center of the undoped GaAs QW region. Atomic force microscopy of an uncapped QD layer confirmed a dot density of $\sim 7 \times 10^8$/cm^2 with a narrow size distribution. The samples were processed into surface emitting LEDs [17,19] and placed in a magneto-optic cryostat. Spin-polarized electrons were electrically injected from the Fe contact into the QDs, and the EL was measured along the surface normal (Faraday geometry) and analyzed for positive and negative helicity (σ^+ and σ^-).

Figure 1(a) shows the QD EL spectra for selected electrical bias conditions, illustrating sequential occupation of the *s*, *p*, *d* and *f* shells with increasing current. Figures 1(b) and 1(c) display the continuous evolution of the shell intensity with bias. Since there is a large dynamic range in the EL intensities, data for the bias ranges 1.7–1.9 and

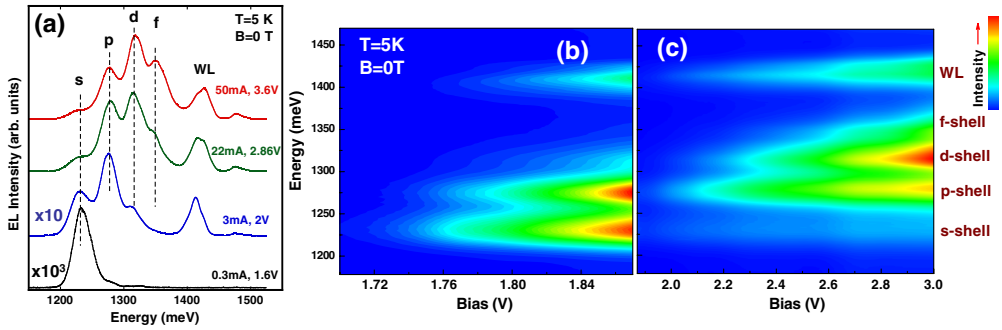

FIG. 1 (color online). (a) EL spectra for selected electrical bias conditions, showing sequential occupation of the QD s, p, d, and f shell states. Contour plot at biases (b) 1.7–1.9 V and (c) 1.9–3.0 V show the gradual filling of the QD shell states.

1.9–3.0 V are plotted separately for clarity. At low bias, only the ground-state s shell is occupied, resulting in a single emission peak at ~1230 meV. The s shell is twofold (spin) degenerate, and can be occupied by two excitons, i.e., electron-hole pairs. Increasing the bias voltage results in continuous filling of the s shell and a corresponding increase and saturation of its emission intensity. At slightly higher bias, emission associated with the p shells appears at 1275 meV, and dominates the EL spectrum from 1.9 to 2.5 V. Further increase of bias results in a gradual filling of the p shell and the appearance of the higher-energy d shell at 1315 meV. Finally, the f shell emerges as a distinct feature (1350 meV) at a bias of ~2.8 V. The highest energy peak (1415 meV) labeled "WL" is due to electron-hole recombination in the InAs two-dimensional wetting layer [19,23]. The sequential occupation of these electronic shells has been observed in optical excitation studies with increasing laser power [8,22] but not with direct control by spin-polarized current injection.

The circular polarization $P_{\mathrm{circ}} = (I_+ - I_-)/(I_+ + I_-)$, for the p, d, and f shell EL intensity peaks is plotted as a function of magnetic field B in Fig. 2(a) for $I = 30$ mA and an applied voltage $V = 3.0$ V. The s shell is not shown because at this bias the polarization at the intensity peak is in the background of the polarization peak B [see Fig. 3(c)]. Here $I_+(I_-)$ is the intensity of the EL analyzed as positive helicity σ_+ (negative helicity σ_-). At zero magnetic field there is no polarization for any of the EL features because the injected electron spin lies in-plane and orthogonal to the hole spins. A magnetic field rotates the Fe magnetization (electron spin) out-of-plane, so that the electron spin is manifested as EL polarization.

The circular polarization at energies corresponding to the intensity peaks of the p and d shells is very low at this bias. This is attributed to the fact that these shells are completely filled, and thus occupied by equal numbers of spin-up and spin-down electrons. In contrast, the polarization of the partially filled f shell is high and its magnetic field dependence exhibits clear evidence of spin injection from Fe, since P_{circ} tracks the out-of-plane magnetization of the Fe contact [17,20,21]. In the inset of Fig. 2(a) we plot the circular polarization of the d shell intensity peak at a lower bias of 1.94 V for comparison where the shell is partially filled (open symbols). In this case, the d shell peak also exhibits high polarization and a field dependence characteristic of spin injection from the Fe, in contrast to the case where it is completely filled (closed symbols).

EL spectra (black lines) taken at $B = 3$ T are plotted in Fig. 3 for $I = 0.32$, 2, and 30 mA. We also plot the circular polarization P_{circ} (solid red lines) of the emitted light as a function of photon energy. A simple model of shell occupation (e.g. one which neglects exchange) would predict that the polarization maxima would coincide with the intensity maxima. This is indeed the case for partially

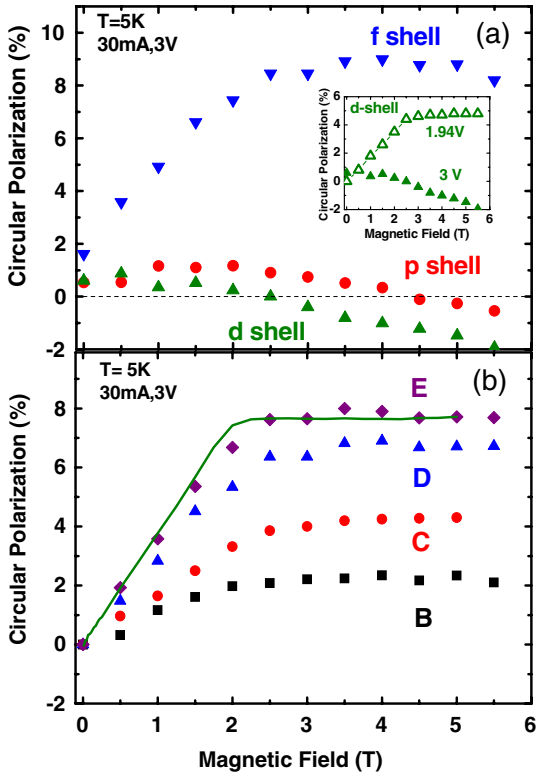

FIG. 2 (color online). P_{circ} vs magnetic field at $T = 5$ K, $I = 30$ mA, $V = 3$ V measured at the (a) EL intensity maxima and (b) polarization maxima (features B, C, D, and E in Fig. 3). The inset shows P_{circ} vs magnetic field for the d shell at two different bias conditions. A weak background of $+0.3\%/T$ was subtracted from the f shell data in (a) and from all data in (b).

occupied shells, as seen in Fig. 3(a) for the p shell, although a small red shift is already evident in the polarization peak. However, in general, the polarization exhibits maxima (labeled A, B, C, D, and E) at energies significantly offset from the EL intensity peaks. The magnetic field dependence of the circular polarization of these features is summarized in Fig. 2(b) for a bias of 3 V and 30 mA. In each case, P_{circ} tracks the magnetization of the Fe contact, shown as a solid line scaled to the data, indicating that the measured polarization is due to polarized electrons injected from the Fe. Feature A is too weak at this bias for reliable polarization measurements. Inverting the field changes the sign of the polarization, as expected. It is evident in Fig. 2(b) that the polarization decreases systematically from f to s shell. One possible interpretation is that as the electrons relax in energy from higher to lower shells, in each step there is a finite probability of spin-flip of the majority electrons resulting in smaller polarization [24]. Another reason for the decrease of polarization could be Fermi blocking [25].

To understand the origin of the strong polarization maxima appearing between the EL intensity peaks, we calculate the emission spectra arising from multiexciton configurations in the QDs using exact diagonalization techniques for up to $N = 6$ electron-hole pairs for (a) unpolarized electrons and holes, and (b) spin-polarized electrons and unpolarized holes. Details of the calculations may be found in Refs. [26,27]. Lateral confinement energies $\Omega_0{}^e = 35$ meV for electrons and $\Omega_0{}^h = 17.5$ meV for holes were used as determined from the experimental intershell energy spacings. In plotting the resulting emission spectra we neglect the energy gap of the QD material.

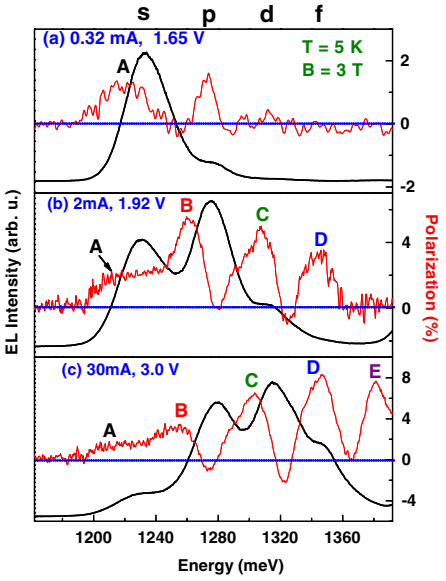

FIG. 3 (color online). EL spectra and P_{circ} vs photon energy at $T = 5$ K, $B = 3$ T with electrical bias of (a) 0.32 mA, 1.65 V, (b) 2 mA, 1.92 V, and (c) 30 mA, 3 V. The thicker black lines are the EL spectra and the solid red lines are the circular polarization.

The lateral confinement of the quantum dot is approximated by a two-dimensional harmonic oscillator (HO) potential, and the eigenenergies and eigenfunctions of the system are determined in the configuration-interaction approach. The emission spectra of the N-exciton system are computed using Fermi's golden rule.

Figure 4(a) shows the calculated emission spectra for $N = 2$, which corresponds to the experimental results of Fig. 3(a) (s shell completely filled, p shell just beginning to be occupied) with the Fe magnetization saturated out-of-plane at $B = 3$ T. In the upper (lower) panel of Fig. 4(a) we show the calculated spectra for unpolarized (spin-polarized) electrons. Injection of spin-polarized electrons forces spin-aligned partial occupation of the next state, in this case the lower lying level of the p shell (doubly degenerate at $B = 0$), labeled p_1. The initial states of multiexciton configurations are shown to the right of Fig. 4(a) for a total QD electron spin of $S_z = 0$ (ground state) and $S_z = -1$ (excited state). For $S_z = 0$, the calculated EL emission feature associated with the filled s shell is unpolarized, i.e., σ^+ and σ^- are equal. For $S_z = -1$ the emission shows two features, a redshifted peak [identified as feature A in Fig. 3(a)] and a blueshifted feature, initially forbidden, which becomes weakly allowed through mixing with higher-energy configurations. There is no clear evi-

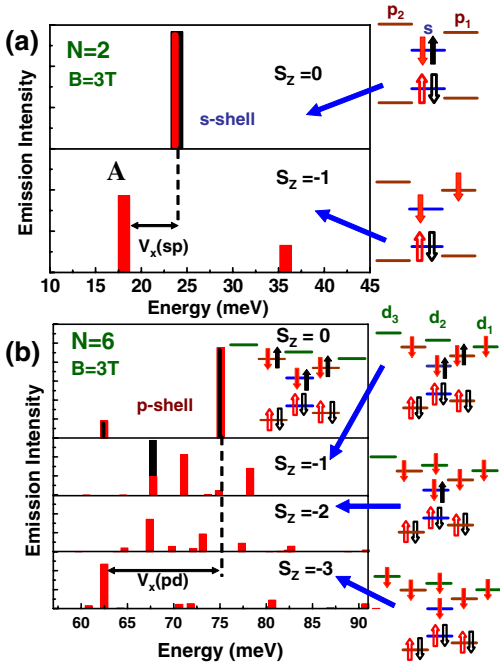

FIG. 4 (color online). Emission spectra calculated in the configuration-interaction approach at magnetic field of 3 T. Emission of the cases of unpolarized (upper panel) and polarized (lower panel) electrons for (a) the biexciton, and (b) the six-exciton system. Black color denotes σ^- polarization while red color denotes σ^+ polarization. The ground-state initial configurations of the system are shown schematically on the right of the figure (blue: s shell, brown: p shell, green: d shell). Closed (open) arrows indicate the spin of the electrons (holes).

dence in our data for the blue-shifted feature due to its low intensity and inhomogeneous broadening of the EL peaks. The peak at 1273 meV in Fig. 3(a) is associated with the emerging p shell EL feature at this bias. At this low occupation the polarization maximum nearly coincides with the p shell EL peak.

For $N = 2$ the experimental value of the redshift of feature A with respect to the s shell is 7 ± 2 meV, in reasonable agreement with the calculated value of 5.7 meV. The calculation shows that this shift is approximately equal to the average exchange energy between electrons in the s and p shells, and we conclude that $V_X(sp)$ is 7 ± 2 meV. Although feature A is predicted to be 100% polarized as σ^+, the experimental data show a much lower polarization. We attribute the low polarization observed to the fact that the electrons injected into the QDs are only partially polarized and thus the experimental data are best described by a convolution of features from both panels of Fig. 4(a) ($S_z = 0$, $S_z = -1$).

Higher bias results in significant occupation of the p shell and partial occupation of the d shell (threefold degenerate at $B = 0$), as shown in Fig. 3(b), producing a larger redshift due to contributions from p-d exchange. The calculated emission spectra in the vicinity of the p shell for six electron-hole pairs per QD ($N = 6$) for $S_z = 0$ (unpolarized electrons) and $S_z = -1$, -2, and -3 (spin-polarized electrons in the s, p, and d shells) are shown in Fig. 4(b). As the total net spin of the confined electrons is increased, the calculation predicts larger redshifts with respect to the p shell energy position. At a bias of 1.92 V, 2 mA [Fig. 3(b)], the s and p shells are completely filled while the d shell has just begun to be occupied. Thus the calculated spectra in Fig. 4(b) can be compared directly with the experimental results shown in Fig. 3(b). Feature B in the experimental data, redshifted by 13.5 ± 1 meV from the p shell intensity peak, is best described as a convolution of the calculated features for $S = -1$, -2, and -3 shown in Fig. 4(b). We point out that the features at 67 meV for $S_z = -1$ and $S_z = -2$ have a near-zero net circular polarization when summed. Thus we expect that the polarization peak labeled B is dominated by the $S_z = -3$ feature at 62.5 meV. The calculated redshift ($\approx$12.9 meV) for this feature is reasonably close to the measured red shift (13.5 meV) of feature B. The calculation shows that this shift is approximately equal to the average exchange energy between electrons in the p and d shells, and we conclude that $V_X(pd)$ for $N = 6$ is 13.5 ± 1 meV. The calculation also predicts the presence of weaker spectral features that are blueshifted with respect to the p shell. The convolution of the blueshifted features in Fig. 4(b) could be associated with the low energy shoulder of feature C appearing around 1292 meV in Fig. 3(b), although an unambiguous identification is not possible.

At a bias of 3 V [Fig. 3(c)], the f shell has just begun to be occupied, leading to an increase in the redshift of the polarization peaks relative to the intensity peaks due to contributions from additional exchange channels (e.g., d-f exchange). However, we cannot extract a value for $V_x(df)$ because the large number of excitons makes this intractable.

In summary, the redshift of the QD shell EL polarization provides a quantitative measure of intershell exchange energies.

Work at NRL supported by ONR through core programs. Work at UB supported by ONR (N000140610174) and NSF (ECCS0824220). Work at IMS NRC supported by the Canadian Institute for Advanced Research, by QuantumWorks, and by a NRC-CNRS research grant.

*gnk@anvil.nrl.navy.mil
jonker@nrl.navy.mil

[1] H. Dery, P. Dalal, L. Cywinski, and L. J. Sham, Nature (London) **447**, 573 (2007).
[2] D. P. DiVincenzo *et al.*, Nature (London) **408**, 339 (2000).
[3] M. Kroutvar *et al.*, Nature (London) **432**, 81 (2004).
[4] S. A. Wolf *et al.*, Science **294**, 1488 (2001).
[5] I. Žutić, J. Fabian, and S. Das Sarma, Rev. Mod. Phys. **76**, 323 (2004).
[6] M. Holub, J. Shin, D. Saha, and P. Bhattacharya, Phys. Rev. Lett. **98**, 146603 (2007).
[7] M. Paillard *et al.*, Phys. Rev. Lett. **86**, 1634 (2001).
[8] M. Bayer *et al.*, Nature (London) **405**, 923 (2000).
[9] P. Hawrylak and M. Korkusinski, in *Single quantum dots: Fundamentals, Applications, and New Concepts*, edited by P. Michler, Topics in Applied Physics (Springer-Verlag, Berlin, 2003), Vol. 90.
[10] B. D. Gerardot *et al.*, Nature (London) **451**, 441 (2008).
[11] M. E. Ware *et al.*, Phys. Rev. Lett. **95**, 177403 (2005).
[12] S. Moriyama *et al.*, Phys. Rev. Lett. **94**, 186806 (2005).
[13] F. Kuemmeth, S. Ilani, D. C. Ralph, and P. L. McEuen, Nature (London) **452**, 448 (2008).
[14] L. He and A. Zunger, Phys. Rev. B **73**, 115324 (2006).
[15] Y. Chye *et al.*, Phys. Rev. B **66**, 201301 (2002).
[16] W. Loffler *et al.*, Appl. Phys. Lett. **88**, 062105 (2006).
[17] C. H. Li *et al.*, Appl. Phys. Lett. **86**, 132503 (2005).
[18] G. Itskos *et al.*, Appl. Phys. Lett. **88**, 022113 (2006).
[19] C. H. Li *et al.*, Appl. Phys. Lett. **91**, 262504 (2007).
[20] A. T. Hanbicki *et al.*, Appl. Phys. Lett. **80**, 1240 (2002).
[21] B. T. Jonker and M. E. Flatte, in *Nanomagnetism: Ultrathin Films, Multilayers and Nanostructures*, edited by D. L. Mills and J. A. C. Bland in Contemporary Concepts of Condensed Matter Science, edited by E. Burstein, M. L. Cohen, D. L. Mills, and P. J. Stiles, (Elsevier, New York, 2006), p. 227.
[22] S. Raymond *et al.*, Phys. Rev. Lett. **92**, 187402 (2004).
[23] P. Offermans *et al.*, Appl. Phys. Lett. **87**, 111903 (2005).
[24] G. A. Narvez, G. Bester, and A. Zunger, Phys. Rev. B **74**, 075403 (2006).
[25] M. Oestreich *et al.*, Phys. Rev. B **53**, 7911 (1996).
[26] P. Hawrylak, Phys. Rev. B **60**, 5597 (1999).
[27] M. Korkusinski and P. Hawrylak, Phys. Rev. Lett. **101**, 027205 (2008).